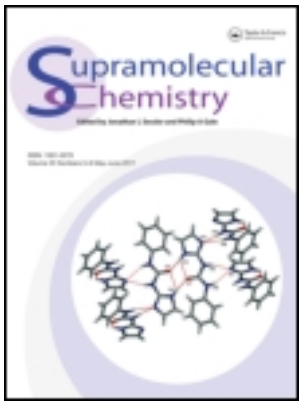

Supramolecular Chemistry
Publication details, including instructions for authors and subscription information:
http://www.tandfonline.com/loi/gsch20

Facile, high-yielding synthesis of deepened cavitands: a synthetic and theoretical study

Zsolt Csók [a], Tamás Kégl [a], László Párkányi [b], Ágnes Varga [c], Sándor Kunsági-Máté [c] & László Kollár [a]

[a] Department of Inorganic Chemistry, University of Pécs, Ifjúság 6, H-7624, Pécs, Hungary

[b] X-ray Diffraction Laboratory, Institute of Structural Chemistry, Chemical Research Center, Hungrian Academy of Science, Pusztaszeri 59-67, H-1025, Budapest, Hungary

[c] Department of General and Physical Chemistry, University of Pécs, Ifjúság 6, H-7624, Pécs, Hungary

Available online: 06 Jul 2011

To cite this article: Zsolt Csók, Tamás Kégl, László Párkányi, Ágnes Varga, Sándor Kunsági-Máté & László Kollár (2011): Facile, high-yielding synthesis of deepened cavitands: a synthetic and theoretical study, Supramolecular Chemistry, 23:10, 710-719

To link to this article: http://dx.doi.org/10.1080/10610278.2011.593633

Supramolecular Chemistry
Vol. 23, No. 10, October 2011, 710–719

Taylor & Francis
Taylor & Francis Group

Facile, high-yielding synthesis of deepened cavitands: a synthetic and theoretical study

Zsolt Csók[a]*, Tamás Kégl[a], László Párkányi[b], Ágnes Varga[c], Sándor Kunsági-Máté[c] and László Kollár[a]

[a]*Department of Inorganic Chemistry, University of Pécs, Ifjúság 6, H-7624 Pécs, Hungary;* [b]*X-ray Diffraction Laboratory, Institute of Structural Chemistry, Chemical Research Center, Hungrian Academy of Science, Pusztaszeri 59-67, H-1025 Budapest, Hungary;* [c]*Department of General and Physical Chemistry, University of Pécs, Ifjúság 6, H-7624 Pécs, Hungary*

(*Received 8 December 2010; final version received 9 May 2011*)

A wide variety of 2-methyl-resorcinol-based deepened cavitands were synthesised from readily available reagents in a four-step procedure with overall yields of up to 62%. A systematic variation of the rim was carried out by building up a flexible upper aromatic wall on the rigid cavitand platform through CH_2, CH_2O and CH_2OCH_2 spacers. These aromatic walls were further extended by a Suzuki cross-coupling reaction. Full characterisation of the synthesised cavitands was carried out. The solid-state structure of tetrakis(phenoxymethyl)cavitand was determined by X-ray crystallography. Gas-phase theoretical calculations for this molecule predict the presence of weak T-shaped interactions between the upper phenyl rings. The host–guest complex formation ability of two deepened cavitand hosts towards 4-chloro-benzotrifluoride was proved by photoluminescence method.

Keywords: supramolecular chemistry; host–guest systems; cavitands; π interactions

1. Introduction

The 'molecule within a molecule' concept was first introduced by Cram (*1*). Since then, there has been an ever growing interest in molecular containers having expanded inner cavities capable of housing sizable or multiple guests. Molecular containers are of particular interest in separation science, drug-delivery systems and molecular sensing and recognition (*2*). Host molecules are able to shield their guests from the exterior solution, which might cause radical changes in their physical and/or chemical properties. This phenomenon was demonstrated well, e.g. in the stabilisation of short-lived reaction species such as cyclobutadiene (*3*). Furthermore, the encapsulation of guest molecules within an extended cage and subsequent release of the products may result in their use as nanosized reactor chambers (*4*).

Several synthetic methodologies were developed to increase the inner volume of molecular containers. The covalent synthesis of the first closed-surface carcerand and its carceplex (*5*) has inspired a number of researchers to prepare structurally well-defined container compounds and determine their host–guest binding properties (*6*). However, these synthetic procedures mostly involve intricate reaction routes that are frequently combined with low isolated yields, which make their application rather limited. Recently, dynamic covalent chemistry has been effectively utilised to overcome such difficulties (*7*). Self-assembly through metal–ligand interactions, van der Waals forces and, mainly, hydrogen bonding also plays an important part in constructing large molecular capsules with increased internal cavities (*8*). On the other hand, these non-covalent systems often suffer from relative instability, functional group intolerance and insolubility in organic solvents.

First-generation cavitands (*9*) based on resorcin[4] arenes (*10*) are conformationally rigid, bowl-shaped molecules, and thus, are ideal platforms for accommodating small molecules, ions or both. Various synthetic strategies have been developed to produce deepened cavitands with an open end. The depth of the cavitands was increased either by Suzuki cross-coupling reactions (*11*) or by bridging the resorcinarene hydroxyl groups with 1,4-diazine derivatives (*12*). The latter family of cavitands was developed further into one of the largest synthetic hosts, which are able to complex extended adamantane and pyridine derivatives of up to 19 Å in length (*13*). Surprisingly, only a few studies utilise the convenient Williamson etherification on the rim of the cavitand skeleton (*14*). Herein, we report a facile, high-yielding synthetic procedure and full characterisation of a novel family of deepened cavitands.

2. Results and discussion

2.1 Synthetic studies

This series of deepened cavitands was synthesised in four simple, high-yielding steps, starting from 2-methylresorcinol and acetaldehyde (Scheme 1). The obtained tetrakis(methyl)resorcin[4]arene (*15*) (**1**) was bridged by

*Corresponding author. Email: zscsok@gmail.com

ISSN 1061-0278 print/ISSN 1029-0478 online

http://dx.doi.org/10.1080/10610278.2011.593633
http://www.tandfonline.com

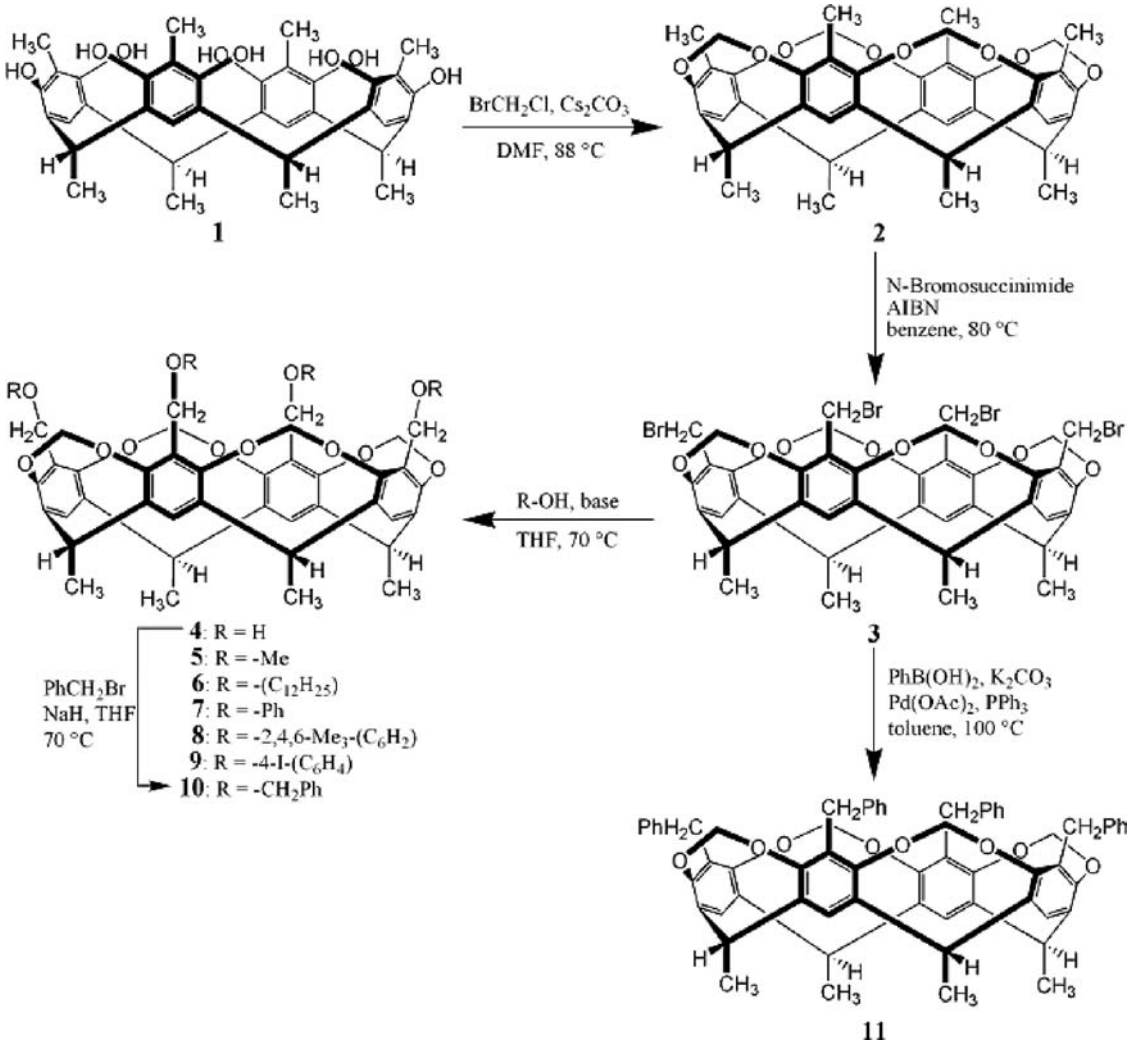

Scheme 1. Synthetic route for the deepened cavitands.

$BrCH_2Cl$ (**2**) (*16*), and selectively brominated according to Sorrell and Pigge (*17*) using azobisisobutyronitrile as a catalyst to afford tetrakis(bromomethyl)cavitand (**3**) in 80% combined yield. Cavitand **3** was then reacted with an excess of various aliphatic alcohols and phenols in the presence of an adequate base to give the corresponding tetrakis(alkoxymethyl) (**5**, **6**, **10**) and tetrakis(aryloxymethyl)cavitands (**7**–**9**) in high (60–78%) isolated yields. These reactions proceeded well at room temperature; however, full etherification was only seen at 70°C after 16 h. Sodium hydroxide was used to deprotonate phenol derivatives, whereas K_2CO_3 was sufficient to carry out the reaction with methanol. Sodium hydride was used for the preparation of **10**. All these cavitands turned out to be pure after carrying out a simple work-up procedure, except for compound **8** that required further purification. Cavitand **3** was also reacted with $PhB(OH)_2$ under typical Suzuki-reaction conditions to yield tetrabenzylcavitand (**11**). The presence of an unidentified minor component made purification by column chromatography inevitable, which dramatically decreased the yield to 24% in this coupling reaction. Compound **9**, bearing four aryl iodide moieties, was used to further extend the aromatic walls of the cavity in a Suzuki cross-coupling reaction (Scheme 2). This reaction provided cavitand **12** with a considerably large, hydrophobic pocket in good yield (59%).

We also describe a simple method for the synthesis of tetrakis(hydroxymethyl)cavitand (**4**). This key intermediate was previously prepared either by $LiAlH_4$ reduction of tetraesters (*5*, *18*) or by hydrolysis of the tetra(acetoxymethyl)cavitand (*19*). Here, we propose NaOH hydrolysis of **3** that affords **4** in excellent yield (81%). Tetrol **4** was used to synthesise **10** using the easily available benzyl bromide derivative (see Section 4, Method B).

All compounds possess a high degree of symmetry (C_4) due to the complete, fourfold etherification, which is reflected in their simple ^1H NMR spectra. The formation of the alkyl(aryl)oxymethyl cavitands was best followed by

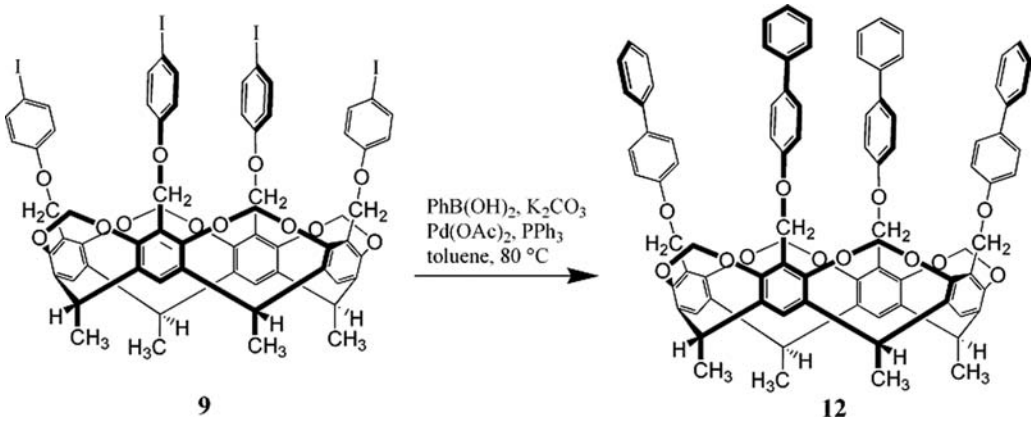

Scheme 2. Synthesis of tetrakis(4-phenyl-phenoxymethyl)cavitand (**12**).

the unique downfield shifts of the methylene-spacer ($ArCH_2O$) protons (Figure 1). Upon carrying out the Suzuki cross-coupling reaction, this singlet resonance was upfield shifted to 3.71 ppm in cavitand **11**. The chemical shifts of the methyleneoxy-bridge (OCH_2O) protons are also characteristic; they appear as a sharp pair of doublets indicating the inherent rigidity of the cavitand framework. All signals of the 'parent' cavitand skeleton are broadened in $CDCl_3$ in the ^1H NMR spectrum of compound **6**, whereas the resonances of the C_{12} alkyl chain remain sharp (Figure 1). However, the observed line broadening disappears upon changing the NMR solvent to DMSO-d_6. Compound **6** bearing long alkyl chains resembles the cavitand obtained by ring-opening metathesis polymerisation of caprolactam (*20*). The structural assignments of this cavitand family were also confirmed by ^{13}C NMR and MALDI-TOF-MS measurements. The matrix [2, 5-dihydroxybenzoic acid (DHB)] and the solvents used contain sodium ions; thus, sodium adducts are commonly detected by MALDI-TOF-MS. The mass shifts were only $[M + 22]^+$ instead of the expected $[M + 23]^+$ due to the difference in the average mass that is always higher than monoisotopic mass, and because of the inhomogeneous matrix/sample mixture layer, which is quite usual with DHB. In these cases, a mass shift of 0.2–0.3 Da was obtained according to the appeared double peaks.

Colourless single crystals of **7** suitable for X-ray crystallography were obtained from a $CHCl_3$/MeOH recrystallisation chamber. The molecular structure of **7** is shown in Figure 2. Dihedral angles formed by the planes of the C1···C6 rings are 76.6° (A/B, A/C, B/D, C/D) and 57.5° (A/D, B/C). Each ring forms two different dihedral angles with its neighbours, i.e. the dihedral angles alternate. The C8···C13 ring planes behave differently. They form identical dihedral angles with their neighbours (83.6°) and a different one across the macrocycle (38.9°). Characteristic torsion angles of the linkers joining the structural units range from 91.4° to 100.9° (Table 1).

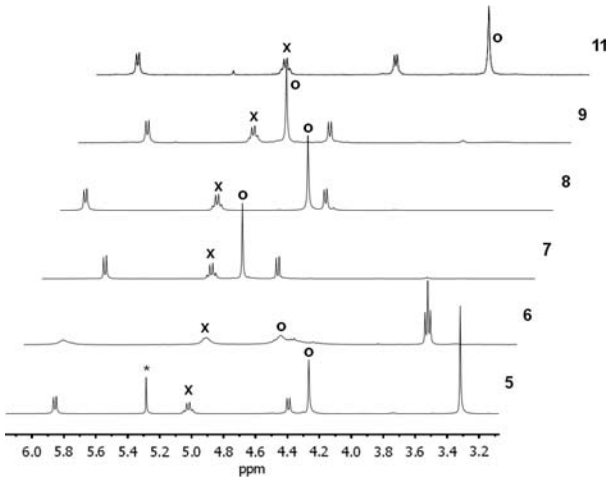

Figure 1. Partial ^1H NMR spectra of **5**–**9** and **11**, ○ and × denote the spacer methylene and methyne protons, respectively (* stands for the residual protons of CH_2Cl_2).

2.2 Theoretical studies

The geometry of compound **7** was optimised at the PBEPBE/6-31G(d,p) level of theory, and the resulting structure is shown in Figure 3. The minimum-energy structure exhibits symmetry very close to C_4. Most of the computed structural parameters (bond length, bond angles and torsion angles) are in reasonable agreement with the X-ray structure of **7**. The deviation from C_{4v} symmetry to C_4 is a consequence of the deviation of dihedral angle (C6—C1—C7—O4) from −90° to −77.8° (−76.4° in the X-ray structure). The rotation of the phenoxy groups around the C1—C7 axis (and the analogous carbon–carbon bonds) results in a subtle change in the bond lengths as well as in the natural population analysis (NPA) charges of the aromatic rings and the OCH_2O bridges of the cavitand skeleton. The C—C distances in the aromatic rings are somewhat elongated compared to 1.403 Å in benzene, optimised at the same level of theory as **7**.

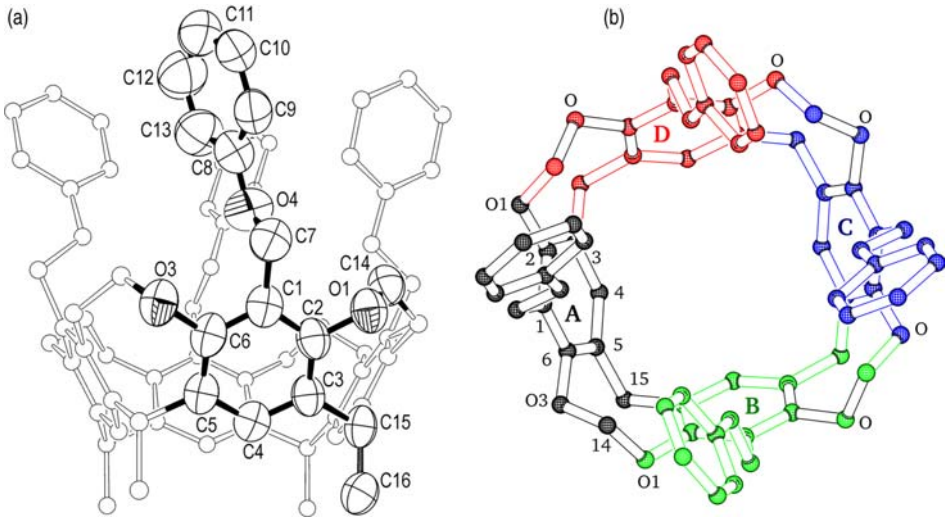

Figure 2. (a) Molecular diagram of **7** with the atomic numbering (hydrogen atoms are omitted for clarity). Atomic displacement ellipsoids represent 40% probabilities. (b) Top view of the molecule. Symmetry generated parts are drawn in green, blue and red colours. Carbon atoms are denoted by bar numbers.

The main difference between the computed and the experimental structures is the significantly closer arrangement of the four phenoxymethyl groups, which can be attributed to weak interactions of the neighbouring rings causing a slight contraction of the C12—C13 bond. In contrast to the T-shaped $\pi-\pi$ interactions described in the literature (*21*), in which the first ring is oriented towards the centre of the second one, these intramolecular interactions can be attributed mainly to the interactions between the inner ortho(or meta)-positioned hydrogen and the ortho (or meta) carbon of the perpendicularly orientated neighbouring ring (see Figure 3). These non-contact distances are estimated to be 3.522 and 3.141 Å, respectively.

The molecular graph of **7** (Figure 4) obtained within the framework of the quantum theory of atoms in molecular (QTAIM) analysis exhibits a cage critical point (CCP), revealing a cage formed by the aromatic rings of the phenoxymethyl substituents. This cage is outlined by the H . . . C interactions between the perpendicular rings forming a four-sided wall, and additionally, an upper and a lower plane having one ring critical point (RCP) for each. Figure 5 shows the Laplacian distribution $\nabla^2\rho(\mathbf{r})$ in the plane of the T-shaped interaction. Several other ring structures are predicted within **7** with another CCP in the centre of the cavitand backbone.

Espinosa et al. (*22*) proposed a simple formula expressing the relationship between the hydrogen bond energy and the local potential energy density $V(\mathbf{r})$ in the bond critical point (BCP) with the proportionality factor being in volume atomic units:

$$E_{HB} = \frac{1}{2}V(\mathbf{r}_{CP}). \quad (1)$$

The local potential energy density $V(\mathbf{r}_{CP})$ can be obtained from the topological parameters using the local

Table 1. Characteristic bond distances (Å) and torsion angles (°).

C1—C2	1.399(7)	C1—C6	1.400(7)
C2—C3	1.376(7)	C5—C6	1.388(7)
C3—C4	1.399(7)	C4—C5	1.398(7)
C2—O1	1.398(6)	C6—O3	1.405(6)
C3—C15	1.536(7)	C15—C16	1.531(7)
O1—C14	1.418(6)	C1—C7	1.509(6)
C7—O4	1.438(5)	O4—C8	1.344
C8—C13	1.390	C13—C12	1.390
C12—C11	1.390	C11—C10	1.390
C10—C9	1.390	C9—C8	1.390
C4—C3—C15—C6[a]	92.5(5)	C4—C5—C15[a]—C3[a]	93.3(5)
C1—C2—O1—C14	98.8(5)	C2—O1—C14—O3[a]	−92.0(5)
O1—C14—O3[a]—C6[a]	91.4(5)	C14—O3[a]—C6[a]—C1[a]	100.9(5)

Note: Atoms marked with *a* indicate neighbouring structural units.

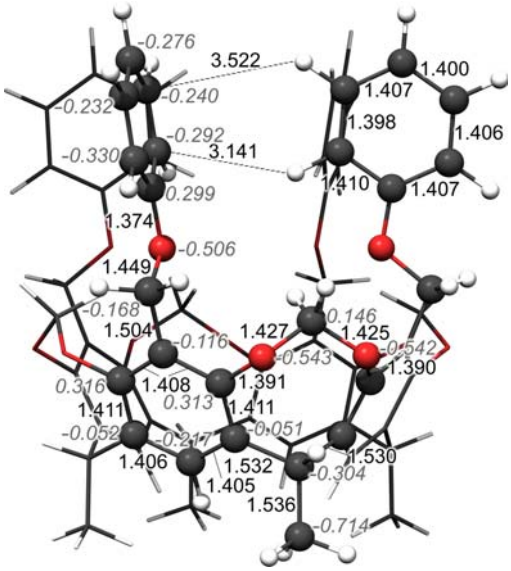

Figure 3. Structure of **7** computed at the PBEPBE/6-31G(d,p) level of theory. Selected bond distances are in Å. NPA charges are in italics.

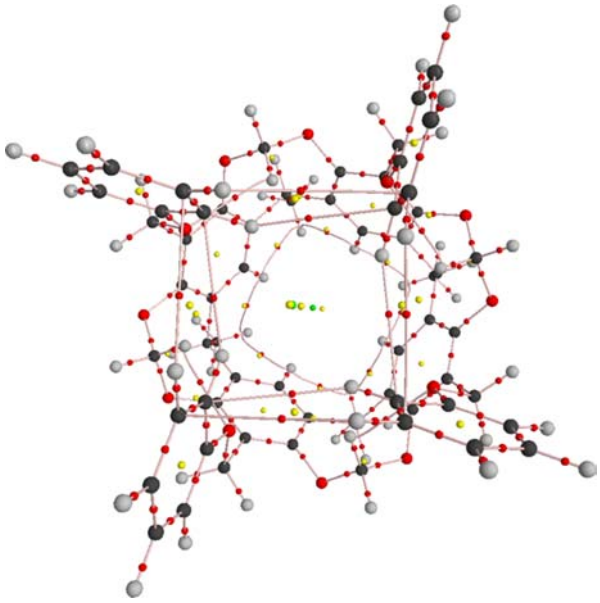

Figure 4. Molecular graph of **7** (top view). The colour scheme identifying the critical points is as follows: red for BCPs; yellow for RCPs and green for CCPs. The nuclear maxima are denoted by larger spheres.

form of the virial equation:

$$V(\mathbf{r}_{CP}) = \frac{\hbar^2}{4m}\nabla^2\rho(\mathbf{r}_{CP}) - 2G(\mathbf{r}_{CP}), \qquad (2)$$

where G is the local electronic kinetic energy density.

Using Equation (1) the interaction energy is estimated to be 0.7 and 1.5 kcal/mol for the C . . . H interactions with distances 3.522 and 3.141 Å, respectively. Thus, the overall stabilisation energy for the T-shaped interactions of the upper aromatic walls is <10 kcal/mol, suggesting that an incoming, appropriate guest molecule can enter the cavity with a low-activation barrier.

2.3 Host–guest complexation studies

As preliminary studies, the host–guest complex formation ability of two deepened cavitand molecules (**7** and **8**) towards 4-chloro-benzotrifluoride (**13**) was investigated by photoluminescence (PL) method in chloroform

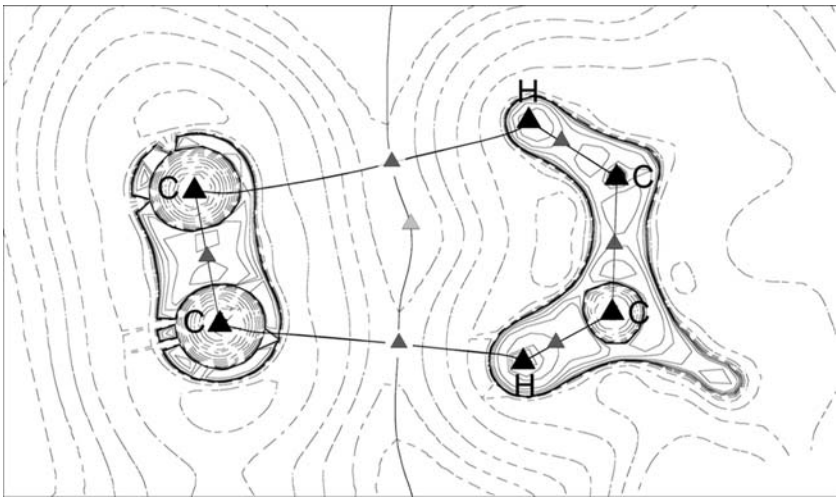

Figure 5. Laplacian distribution of **7** illustrating the 'T-shaped' interaction between two phenyl rings. Solid lines indicate charge concentrations ($\nabla^2\rho(\mathbf{r}) < 0$), whereas dashed lines ($\nabla^2\rho(\mathbf{r}) > 0$) show charge depletions. BCPs are indicated by dark grey, whereas the RCP is light grey. Bond paths (lines of maximum electron density) linking nuclei and zero-flux surfaces (which partition the molecule into its constituent atoms) are designated with solid lines.

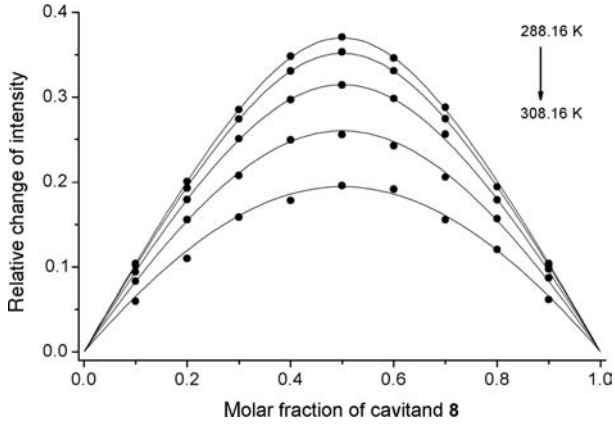

Figure 6. Job's plot of the interaction of host **8** with 4-chlorobenzotrifluoride (**13**).

(see Section 4). The Benesi–Hildebrand method combined with the van't Hoff theory was applied to calculate the thermodynamic parameters of the molecular association. The results justified the presence of the host–guest complexes in solution with considerable concentration and possessing 1:1 stoichiometry. Figure 6 shows Job's plot of the interaction of host **8** with **13**. However, our experiments show significantly different thermodynamics for the complex formation. Although these host–guest interactions are associated with almost the same Gibbs-free energy changes at room temperature ($\Delta G = -26.8$ kJ/mol for **7**:**13** and $\Delta G = -27.2$ kJ/mol for **8**:**13**, respectively), the enthalpy change is much higher when the complex of **7** is formed ($\Delta H = -36.8$ kJ/mol for **7**:**13** and $\Delta H = -29.2$ kJ/mol for **8**:**13**, respectively). The entropy changes were found to be considerably different ($\Delta S = -33.5$ J/K mol for **7**:**13** and $\Delta S = -6.7$ J/K mol for **8**:**13**, respectively). The well-known enthalpy–entropy compensation may be responsible for this unexpected phenomenon, which is probably due to the steric hindrance of the methyl groups located on the upper phenyl rings of compound **8**. The stability constants K_{ass} at room-temperature were determined to be 4.9×10^5 dm^3/mol for **7**:**13** and 5.8×10^5 dm^3/mol for **8**:**13** complexes, respectively.

3. Conclusions

In sum, Williamson etherification provides easy access to a wide variety of deepened cavitands from readily available, inexpensive alcohols. The synthesised cavitands exhibit high stability and good solubility in most organic solvents. The upper aromatic walls are attached to a rigid cavitand platform through CH_2, CH_2O and CH_2OCH_2 spacers. Hence, this 'upper cavity' of the molecule possesses some flexibility, which allows potential guest molecules to enter and to be more or less surrounded by the walls of the host. In this way, the entrapment of guest molecules and their isolation from the bulk medium can be more effective. Theoretical calculations suggest that the formation of a host–guest complex might take place via a small activation barrier. This novel series of deepened cavitands may be useful for complexing electron-poor aromatics, such as nitroaromatics, benzotrifluorides, and so on due to the presence of a flexible binding pocket with tunable electron density. Indeed, two of these deepened cavitands (**7** and **8**) behave as hosts and show the formation of 1:1 complexes with 4-chloro-benzotrifluoride as a guest. Furthermore, cavitand **9**, bearing four aryl iodide moieties, may serve as a potential intermediate for further functionalisation of this cavitand family, as demonstrated in the synthesis of cavitand **12**.

4. Experimental

4.1 General procedures and materials

All reagents and solvents were purchased from Aldrich (Budapest, Hungary). For the synthesis of **10**, tetrahydrofuran (THF) was distilled from sodium/benzophenone under argon atmosphere, and the reaction was carried out under Ar by using standard Schlenk-techniques. General work-up procedure is as follows: the reaction mixture was partitioned between CH_2Cl_2 (30 ml) and water (30 ml). The organic phase was separated, and the aqueous phase was extracted with another portion of CH_2Cl_2 (30 ml). The combined organic phases were washed with water (2×30 ml), dried over $MgSO_4$ and evaporated to dryness. The residue was treated with MeOH, and the resulting precipitate was collected by filtration. ^{1}H and ^{13}C NMR spectra were recorded at 25°C in $CDCl_3$ on a Varian Inova 400 spectrometer at 400.13 and 100.62 MHz, respectively. The ^{1}H and ^{13}C chemical shifts (δ), reported in parts per million (ppm) downfield, are referenced to residual $CHCl_3$ (7.26 ppm) and to the carbon resonance of $CDCl_3$ (77.00 ppm), respectively. MALDI-TOF spectra were obtained on an Autoflex II TOF/TOF spectrometer (Bruker Daltonics, Bremen, Germany) in positive ion modes, using a 337 nm pulsed nitrogen laser (accelerating voltage: 20.0 kV, matrix: DHB).

4.2 Crystallography

CCDC-795580 contains the supplementary crystallographic data for this paper. These data can be obtained free of charge from The Cambridge Crystallographic Data Centre via www.ccdc.cam.ac.uk/data_request/cif.

Crystal data: $C_{64}H_{56}O_{12}$; MW: 1017.09; colourless; block size: $0.37 \times 0.35 \times 0.35$ mm; tetragonal space group P_4/ncc (No. 130); $a = 15.4744(13)$ Å; $c = 25.423(2)$ Å; $V = 6087.7(9)$ Å^3; $Z = 4$; $D_x = 1.110$ g cm^{-3}; $\mu = 0.076$ mm^{-1}; $F(0\,0\,0) = 2144$.

Data collection: Intensity data were collected on a Rigaku R-Axis Rapid diffractometer with Mo-K_α radiation

($\lambda = 0.71075$ Å) at room temperature. A total of 46,012 reflections were collected of which 1602 were unique, $R_{int} = 0.067$. Numerical absorption correction (*23*) was applied to the data (the minimum and maximum transmission factors were 0.975 and 0.986). The crystals diffract poorly, and the resolution of the data is limited to 1 Å.

Structure solution and refinement: The structure was solved with direct methods and refined by anisotropic full-matrix least-squares refinement (*24*) on F^2. Hydrogen positional coordinates were calculated from assumed geometries and were not refined. Difference electron density maps indicate the presence of highly disordered solvent molecules. The SQUEEZE procedure of program PLATON (*25*) was applied, and the solvent-free data were used in further refinement cycles (solvent accessible volume 1309.0 Å^3, total electron count 162 e). Atoms of the C8···C13 phenyl ring were fitted to a regular hexagon and treated as a rigid group throughout the refinement. A total of 1602 reflections were used for the refinement of 158 parameters ($R = 0.1043$, $wR2 = 0.2403$ for all intensity data; $R = 0.0798$, $wR2 = 0.2189$ for 1332 [$I > 2s(I)$], goodness of fit = 1.10). The minimum and maximum final residual electron density was -0.23, 0.18 eÅ^{-3}. A cavity of 2.34 Å radius is inside the cavitand moiety (the centre of the sphere is at 0.250, 0.250 and 0.400). The whole molecule was generated by the 1/2 − *y*,*x*,*z*; 1/2 − *x*, 1/2 − *y*,*z* and *y*,1/2 − *x*,*z* symmetry operations (Figure 2).

4.3 Synthetic procedures

4.3.1 Tetrakis(hydroxymethyl)cavitand (**4**)

To the THF (30 ml) solution of 1 g (1.04 mmol) of **3**, 30 ml of 1 M aqueous NaOH solution was added. The reaction mixture was stirred at 70°C for 48 h. The reaction mixture was partitioned between CH_2Cl_2 (60 ml) and water (30 ml). The organic phase was separated, and the aqueous phase was extracted with another portion of CH_2Cl_2 (30 ml). The combined organic phases were washed with 0.5% aq. HCl solution (30 ml), water (60 ml) and dried over $MgSO_4$. Evaporation of the solvent yielded a light yellow solid ($m = 600$ mg, 81%).

^{1}H NMR ($CDCl_3$): 1.77 (d, $J = 6.9$ Hz, 12H, CH_3CH); 4.44 (d, $J = 6.8$ Hz, 4H, inner of OCH_2O); 4.54 (s, 8H, ArCH_2O); 5.03 (q, $J = 6.9$ Hz, 4H, CHCH$_3$); 5.91 (d, $J = 6.8$ Hz, 4H, outer of OCH_2O); 7.26 (s, 4H, Ar). ^{13}C NMR ($CDCl_3$): 16.02 (CH_3CH); 31.09 (CH$_3$$CH$); 55.36 ($CH_2$OH); 99.67 ($OCH_2O$); 119.61; 126.25; 139.03; 153.10. MS: 735.17 $[M + 22]^+$.

4.3.2 Tetrakis(methoxymethyl)cavitand (**5**)

To the THF (15 ml) solution of 300 mg (0.31 mmol) of **3**, 10 ml of MeOH and 689 mg (4.96 mmol) of K_2CO_3 were added. The reaction mixture was stirred at 70°C for 16 h. General work-up procedure, white solid ($m = 185$ mg, 78%).

^{1}H NMR ($CDCl_3$): 1.75 (d, $J = 7.5$ Hz, 12H, CH_3CH); 3.32 (s, 12H, OCH_3); 4.27 (s, 8H, ArCH_2O); 4.39 (d, $J = 7.2$ Hz, 4H, inner of OCH_2O); 5.02 (q, $J = 7.5$ Hz, 4H, $CHCH_3$); 5.85 (d, $J = 7.2$ Hz, 4H, outer of OCH_2O); 7.25 (s, 4H, Ar). ^{13}C NMR ($CDCl_3$): 16.04 (CH_3CH); 31.06 (CH_3CH); 58.45 (OCH_3); 64.38 (ArCH_2O); 99.52 (OCH_2O); 119.86; 123.89; 138.70; 153.54. MS: 791.24 $[M + 22]^+$.

4.3.3 Tetrakis(dodecanoxymethyl)cavitand (**6**)

To the THF (10 ml) solution of 881 mg (4.73 mmol) of 1-dodecanol, 5 ml of 0.95 M aqueous NaOH solution was added, and was left stirring for 30 min. This solution was then slowly added to the THF (10 ml) solution of 285 mg (0.3 mmol) of **3**. The reaction mixture was stirred at 70°C for 16 h. General work-up procedure, white solid ($m = 249$ mg, 60%).

^{1}H NMR ($CDCl_3$): 0.88 (t, $J = 6.8$ Hz, 12H); 1.26 (br m, 72H); 1.56 (quint, $J = 6.8$ Hz, 8H); 1.76 (d, $J = 6.8$ Hz, 12H, CH_3CH); 3.63 (t, $J = 6.8$ Hz, 8H, OCH_2R); 4.56 (br m, 12H, outer of OCH_2O overlapping with ArCH_2O); 5.03 (br s, 4H, $CHCH_3$); 5.91 (br s, 4H, outer of OCH_2O); 7.25 (s, 4H, Ar). ^{13}C NMR ($CDCl_3$): 14.08; 16.04 (CH_3CH); 22.67; 25.74; 29.33; 29.42; 29.60 (triple intensity); 29.70; 31.13 (CH_3CH); 31.90; 32.81; 55.37 (ArCH_2O); 63.09; 99.74 (OCH_2O); 119.62; 126.35; 139.05; 153.21.

4.3.4 Tetrakis(phenoxymethyl)cavitand (**7**)

To the THF (10 ml) solution of 200 mg (0.21 mmol) of **3**, 2 ml of 1 M aqueous solution of NaOPh (freshly prepared from phenol and NaOH) was added. The reaction mixture was stirred at 70°C for 16 h. General work-up procedure, white solid ($m = 160$ mg, 75%).

^{1}H NMR ($CDCl_3$): 1.83 (d, $J = 7.4$ Hz, 12H, CH_3CH); 4.69 (d, $J = 7.3$ Hz, 4H, inner of OCH_2O); 4.91 (s, 8H, ArCH_2O); 5.10 (q, $J = 7.4$ Hz, 4H, $CHCH_3$); 5.77 (d, $J = 7.3$ Hz, 4H, outer of OCH_2O); 6.94 (m, 12H, Ph); 7.25 (m, 8H, Ph); 7.40 (s, 4H, Ar). ^{13}C NMR ($CDCl_3$): 16.19 (CH_3CH); 31.22 (CH_3CH); 60.45 (ArCH_2O); 100.10 (OCH_2O); 114.58; 120.50; 121.01; 122.77; 129.51; 138.90; 154.04; 158.71. MS: 1039.20 $[M + 22]^+$.

4.3.5 Tetrakis(mesytoxymethyl)cavitand (**8**)

To the THF (10 ml) solution of 920 mg (6.76 mmol) of 2,4,6-trimethylphenol, 10 ml of 0.68 M aqueous NaOH solution was added, and was left stirring for 30 min. This light-violet solution was then slowly added to the THF (10 ml) solution of 400 mg (0.41 mmol) of **3**. The reaction mixture was stirred at 70°C for 16 h. General work-up

procedure, white solid ($m = 350$ mg, 72%). An analytically pure sample was obtained by column chromatography (silica gel; eluent:benzene, $R_f = 0.51$).

^{1}H NMR ($CDCl_3$): 1.85 (d, $J = 7.4$ Hz, 12H, CH_3CH); 2.22 (s, 12H, $ArCH_3$); 2.27 (s, 24H, $ArCH_3$); 4.50 (d, $J = 7.2$ Hz, 4H, inner of OCH_2O); 4.61 (s, 8H, $ArOCH_2$); 5.18 (q, $J = 7.4$ Hz, 4H, $CHCH_3$); 6.00 (d, $J = 7.2$ Hz, 4H, outer of OCH_2O); 6.81 (s, 8H, Ar); 7.42 (s, 4H, Ar). ^{13}C NMR ($CDCl_3$): 16.17 (CH_3CH); 16.24 ($ArCH_3$); 20.57 ($ArCH_3$); 31.31 (CH_3CH); 64.19 (OCH_2); 100.20 (OCH_2O); 120.49; 122.96; 129.54; 130.74; 133.47; 139.24; 153.29; 153.98. MS: 1207.68 $[M + 22]^+$.

4.3.6 Tetrakis(4-iodo-phenoxymethyl)cavitand (**9**)

To the THF (10 ml) solution of 740 mg (3.36 mmol) of 4-iodophenol, 10 ml of 0.34 M aqueous NaOH solution was added, and was left stirring for 30 min. This solution was then slowly added to the THF (10 ml) solution of 200 mg (0.21 mmol). The reaction mixture was stirred at 70°C for 16 h. General work-up procedure, white solid ($m = 215$ mg, 67%).

^{1}H NMR ($CDCl_3$): 1.81 (d, $J = 7.4$ Hz, 12H, CH_3CH); 4.59 (d, $J = 7.3$ Hz, 4H, inner of OCH_2O); 4.86 (s, 8H, $ArCH_2O$); 5.07 (q, $J = 7.4$ Hz, 4H, $CHCH_3$); 5.73 (d, $J = 7.3$ Hz, 4H, outer of OCH_2O); 6.66 (d, $J = 8.7$ Hz, 8H, Ar); 7.38 (s, 4H, Ar); 7.54 (d, $J = 8.7$ Hz, 8H, Ar). ^{13}C NMR ($CDCl_3$): 16.13 (CH_3CH); 31.20 (CH_3CH); 60.62 (OCH_2); 83.30; 99.95 (OCH_2O); 116.84; 120.71; 122.31; 138.39; 138.95; 153.93; 158.44. MS: 1542.77 $[M + 22]^+$.

4.3.7 Tetrakis(benzyloxymethyl)cavitand (**10**)

Method A: To the THF (10 ml) solution of 0.26 ml (2.5 mmol) of benzyl alcohol, 100 mg (2.5 mmol) of 60% NaH was added, and the mixture was left stirring for 30 min. Then, THF (10 ml) solution of 300 mg (0.31 mmol) of **3** was slowly added. The reaction mixture was stirred at 70°C for 16 h and it was poured into 30 ml 0.1 N HCl. Then 30 ml of CH_2Cl_2 was added, the organic phase was separated and the aqueous phase was extracted with another portion of CH_2Cl_2 (30 ml). The combined organic phases were washed with water (2×30 ml), dried over $MgSO_4$ and evaporated to dryness. The residue was treated with MeOH, and the resulting precipitate was collected by filtration. White solid, $m = 230$ mg (69%).

Method B: To the THF (10 ml) solution of 200 mg (0.28 mmol) of **4**, 90 mg (2.24 mmol) of 60% NaH was added, and the mixture was left stirring for 30 min. Then 0.27 ml (2.24 mmol) of benzyl bromide was slowly added. The reaction mixture was stirred at 70°C for 16 h. Work-up as described in Method A. White solid, $m = 160$ mg (53%).

^{1}H NMR ($CDCl_3$): 1.74 (d, $J = 7.3$ Hz, 12H, CH_3CH); 4.28 (m, 12H, $ArCH_2O$ overlapped with inner of OCH_2O); 4.47 (s, 8H, OCH_2Ph); 5.00 (q, $J = 7.3$ Hz, 4H, $CHCH_3$); 5.60 (d, $J = 7.1$ Hz, 4H, outer of OCH_2O); 7.20–7.40 (m, 24H, Ar and Ph). ^{13}C NMR ($CDCl_3$): 16.10 (CH_3CH); 31.11 (CH_3CH); 61.72 ($ArCH_2O$), 72.85 (OCH_2Ph), 99.53 (OCH_2O); 119.88; 123.84; 127.76; 128.32 (double intensity); 130.09; 138.71; 153.72. MS: 1095.53 $[M + 22]^+$.

4.3.8 Tetrabenzylcavitand (**11**)

To the toluene (60 ml) solution of 1.04 g (1 mmol) of **3**, under Ar atmosphere 12 mg (0.05 mmol) of $Pd(OAc)_2$, 28 mg (0.1 mmol) of PPh_3, 1.15 g (8.3 mmol) of K_2CO_3 and 760 mg (6.2 mmol) of $PhB(OH)_2$ were added. The reaction mixture was vigorously stirred at 100°C for 16 h. After cooling, it was filtered through a layer of Celite, and evaporated to dryness. Column chromatography (silica gel; eluent:benzene/*n*-hexane = 4:1, $R_f = 0.64$) yielded the product as white solid (229 mg, 24%).

^{1}H NMR ($CDCl_3$): 1.72 (d, $J = 7.4$ Hz, 12H, CH_3CH); 3.71 (s, 8H, $ArCH_2Ph$); 4.29 (d, $J = 6.9$ Hz, 4H, inner of OCH_2O); 4.98 (q, $J = 7.4$ Hz, 4H, $CHCH_3$); 5.90 (d, $J = 6.9$ Hz, 4H, outer of OCH_2O); 7.15–7.26 (m, 24H, Ar and Ph). ^{13}C NMR (CD_2Cl_2): 19.66 (CH_3CH); 31.66 ($ArCH_2Ar$); 32.14 (CH_3CH); 99.86 (OCH_2O); 119.33; 126.67; 127.35; 128.85; 129.19; 139.74; 141.01; 153.49. MS: 975.50 $[M + 22]^+$; 953.44 $[M]^+$.

4.3.9 Tetrakis(4-phenyl-phenoxymethyl)cavitand (**12**)

To the toluene (20 ml) solution of 380 mg (0.25 mmol) of **9**, under Ar atmosphere 2.9 mg (0.013 mmol) of $Pd(OAc)_2$, 6.8 mg (0.026 mmol) of PPh_3, 276 mg (2 mmol) of K_2CO_3 and 183 mg (1.5 mmol) of $PhB(OH)_2$ were added. The reaction mixture was vigorously stirred at 80°C for 2 days. After cooling, it was filtered through a layer of Celite, and evaporated to dryness. The residue was treated with MeOH, and the resulting precipitate was collected by filtration (195 mg, 59%).

^{1}H NMR ($CDCl_3$): 1.85 (d, $J = 7.4$ Hz, 12H, CH_3CH); 4.73 (d, $J = 7.3$ Hz, 4H, inner of OCH_2O); 4.97 (s, 8H, $ArCH_2Ph$); 5.12 (q, $J = 7.4$ Hz, 4H, $CHCH_3$); 5.82 (d, $J = 7.3$ Hz, 4H, outer of OCH_2O); 6.99 (d, $J = 8.5$ Hz, 8H, Ph); 7.27–7.53 (m, 32H, Ar and Ph). ^{13}C NMR (CD_2Cl_3): 16.20 (CH_3CH); 31.26 (CH_3CH); 60.66 ($ArCH_2O$); 100.17 (OCH_2O); 114.89; 120.62; 122.78; 126.65; 128.17; 128.70; 134.12; 138.95; 140.55; 154.08; 158.25. MS: 1343.41 $[M + 22]^+$.

4.4 Computational details

The geometry of **7** was calculated without any symmetry constraints using the gradient-corrected exchange functional developed by Perdew et al. (*26*) in combination with a correlation functional, developed also by the same

authors, and denoted as PBEPBE. The 6-31G(d,p) basis set (*27*) was used throughout this study. For the stationary point, the Hessian was evaluated to characterise the genuine minimum (no imaginary frequency). NPA and natural bond orbital analysis (*28*) were carried out at the same level of theory as the one used for geometry optimisation. For the calculations, the Gaussian 03 suite of programs was used (*29*). QTAIM analysis of the wave function was carried out with the AIM2000 software (*30*) to investigate the electron density of the optimised structure.

4.5 Host–guest complexation experiments

The host–guest complex formation ability of two deepened cavitands (**7** and **8**) towards 4-chloro-benzotrifluoride (**13**) was investigated using PL method in chloroform. Samples containing 10^{-4} M of **7** or **8** were prepared for these experiments, and the PL spectra of the host molecules were recorded both in the absence and in the presence of 4-chloro-benzotrifluoride as a guest. The concentration of the guest was varied from 1×10^{-4} M up to 9×10^{-4} M through 1×10^{-4} M steps. The samples were excited at 395 nm and the PL peak of the host obtained at 430 nm was used for data evaluation. A highly sensitive Fluorolog τ3 spectrofluorometric system (Jobin-Yvon/SPEX) was used for data collection; a photon counting method with 0.2 s integration time was applied. Excitation and emission bandwidths were set to 1 nm. One millimetre layer thickness of the fluorescent probes with front face detection was used to eliminate the inner filter effect. The stoichiometry of the formed complexes was checked by Job's method. The Benesi–Hildebrand method was used to determine the stability constants at all temperatures (*31*). The van't Hoff theory was applied to calculate the thermodynamic parameters of the interactions.

Acknowledgements

This work was supported by Science, Please! Research Team on Innovation (SROP-4.2.2/08/1/2008-0011). Z.C. and T.K. thank the Bolyai Grants of the Hungarian Academy of Sciences. The authors also thank the Supercomputer Center of the National Information Infrastructure Development (NIIF) Program, and L. Márk (University of Pécs) for carrying out the MS experiments.

References

(1) Cram, D.J. *Nature* **1992**, *356*, 29–36.
(2) Cram, D.J.; Cram, J.M. *Container Molecules and their Guests*; Royal Society of Chemistry: Cambridge, 1994.
(3) Cram, D.J.; Tanner, M.E.; Thomas, R. *Angew. Chem. Int. Ed. Engl.* **1991**, *30*, 1024–1027.
(4) Vriezema, D.M.; Aragones, M.C.; Elemans, J.A.A.W.; Cornelissen, J.J.L.M.; Rowan, A.E.; Nolte, R.J.M. *Chem. Rev.* **2005**, *105*, 1445–1489.
(5) (a) Cram, D.J.; Karbach, S.; Kim, Y.H.; Baczynskyj, L.; Kalleymeyn, G.W. *J. Am. Chem. Soc.* **1985**, *107*, 2575–2576; (b) Cram, D.J.;; Karbach, S.; Kim, Y.H.; Baczynskyj, L.; Marti, K.; Sampson, R.M.; Kalleymeyn, G.W. *J. Am. Chem. Soc.* **1988**, *110*, 2554–2560.
(6) (a) Warmuth, R.; Yoon, J. *Acc. Chem. Res.* **2001**, *34*, 95–105; (b) Jasat, A., Sherman, J.C. Chem. Rev. 1999, *99*, 931–967.
(7) Liu, X.; Warmuth, R. *J. Am. Chem. Soc.* **2006**, *128*, 14120–14127.
(8) (a) Heinz, T.; Rudkevich, D.M.; Rebek, J., Jr. *Angew. Chem. Int. Ed. Engl.* **1999**, *38*, 1136–1139; (b) MacGillivray, L.R.; Atwood, J.L. *Nature* **1997**, *389*, 469–472; (c) Cave, G.W.V.; Ferrarelli, M.C.; Atwood, J.L. *Chem. Commun.* **2005**, 2787–2789; (d) MacGillivray, L.R.; Diamente, P.R.; Reid, J.L.; Rippmeester, J.A. *Chem. Commun.* **2000**, 359–360; (e) Botta, B.; Cassani, M.; D'Acquarica, I.; Subissati, D.; Zappia, G.; Delle Monache, G. *Curr. Org. Chem.* **2005**, *9*, 1167–1202.
(9) (a) Moran, J.R.; Karbach, S.; Cram, D.J. *J. Am. Chem. Soc.* **1982**, *104*, 5826–5828; (b) Cram, D.J., Karbach, S., Kim, H.E., Knobler, C.B., Maverick, E.F., Ericson, J.L., Helgeson, R.C. *J. Am. Chem. Soc.* **1988**, *110*, 2229–2237.
(10) Timmerman, P.; Verboom, W.; Reinhoudt, D.N. *Tetrahedron* **1996**, *52*, 2663–2704.
(11) (a) Ma, S.; Rudkevich, D.M.; Rebek, J., Jr. *J. Am. Chem. Soc.* **1998**, *120*, 4977–4981; (b) Aakeröy, C.B.; Schultheiss, N.; Desper, J. *Org. Lett.* **2006**, *12*, 2607–2610.
(12) (a) Moran, J.R.; Ericson, J.L.; Dalcanale, E.; Bryant, J.A.; Knobler, C.B.; Cram, D.J. *J. Am. Chem. Soc.* **1991**, *113*, 5707–5714; (b) Tucci, F.C.; Rudkevich, D.M.; Rebek, J., Jr. *J. Org. Chem.* **1999**, *64*, 4555–4559.
(13) (a) Starnes, S.D.; Rudkevich, D.M.; Rebek, J., Jr. *J. Am. Chem. Soc.* **2001**, *123*, 4659–4669; (b) Tucci, F.C.; Renslo, A.R.; Rudkevich, D.M.; Rebek, J., Jr. *Angew. Chem. Int. Ed.* **2000**, *39*, 1076–1079.
(14) (a) Barrett, E.S.; Irwin, J.L.; Picker, K.; Sherburn, M.S. *Austr. J. Chem.* **2002**, *55*, 319–325; (b) Boerrigter, H.; Verboom, W.; van Hummel, G.J.; Harkema, S.; Reinhoudt, D.N. *Tetrahedron Lett.* 1996, *37*, 5167-5170.
(15) Tunstad, L.M.; Tucker, J.A.; Dalcanale, E.; Weiser, J.; Bryant, J.A.; Sherman, J.C.; Helgeson, R.C.; Knobler, C.B.; Cram, D.J. *J. Org. Chem.* **1989**, *54*, 1305–1312.
(16) Roman, E.; Peinador, C.; Mendoza, S.; Kaifer, A.E. *J. Org. Chem.* **1999**, *64*, 2577–2578.
(17) Sorrell, T.N.; Pigge, F.C. *J. Org. Chem.* **1993**, *58*, 784–785.
(18) Dueno, E.E.; Bisht, K.S. *Tetrahedron* **2004**, *60*, 10859–10868.
(19) Pellet-Rostaing, S.; Nicod, L.; Chitry, F.; Lemaire, M. *Tetrahedron Lett.* **1999**, *40*, 8793–8796.
(20) Wu, R.; Al-Azemi, T.F.; Bisht, K.S. *Chem. Commun.* **2009**, 1822–1824.
(21) Hobza, P.; Selzle, H.L.; Schlag, E.W. *J. Am. Chem. Soc.* **1994**, *116*, 3500–3506.
(22) Espinosa, E.; Molins, E.; Lecomte, C. *Chem. Phys. Lett.* **1998**, *285*, 170–173.
(23) Higashi, T. *NUMABS, rev. 2002*; Rigaku/MSC, Inc., 1998.
(24) Sheldrick, G.M. *Acta Cryst.* **2008**, *A64*, 112–122.
(25) Spek, A.L. *J. Appl. Cryst.* **2003**, *36*, 7–13.
(26) Perdew, J.P.; Burke, K.; Ernzerhof, M. *Phys. Rev. Lett.* **1996**, *77*, 3865–3868.

(27) Hehre, W.J.; Ditchfield, R.; Pople, J.A. *J. Chem. Phys.* **1972**, *56*, 2257–2261.
(28) Glendening, E.D.; Reed, A.E.; Carpenter, J.E.; Weinhold, F. NBO Version 3.1.
(29) Frisch, M.J.; Trucks, G.W.; Schlegel, H.B.; Scuseria, G.E.; Robb, M.A.; Cheeseman, J.R.; Montgomery, J.A. Jr.; Vreven, T.; Kudin, K.N.; Burant, J.C.; Millam, J.M.; Iyengar, S.S.; Tomasi, J.; Barone, V.; Mennucci, B.; Cossi, M.; Scalmani, G.; Rega, N.; Petersson, G.A.; Nakatsuji, H.; Hada, M.; Ehara, M.; Toyota, K.; Fukuda, R.; Hasegawa, J.; Ishida, M.; Nakajima, T.; Honda, Y.; Kitao, O.; Nakai, H.; Klene, M.; Li, X.; Knox, J.E.; Hratchian, H.P.; Cross, J.B.; Adamo, C.; Jaramillo, J.; Gomperts, R.; Stratmann, R.E.; Yazyev, O.; Austin, A.J.; Cammi, R.; Pomelli, C.; Ochterski, J.W.; Ayala, P.Y.; Morokuma, K.; Voth, G.A.; Salvador, P.; Dannenberg, J.J.; Zakrzewski, V.G.; Dapprich, S.; Daniels, A.D.; Strain, M.C.; Farkas, O.; Malick, D.K.; Rabuck, A.D.; Raghavachari, K.; Foresman, J.B.; Ortiz, J.V.; Cui, Q.; Baboul, A.G.; Clifford, S.; Cioslowski, J.; Stefanov, B.B.; Liu, G.; Liashenko, A.; Piskorz, P.; Komaromi, I.; Martin, R.L.; Fox, D.J.; Keith, T.; Al-Laham, M.A.; Peng, C.Y.; Nanayakkara, A.; Challacombe, M.; Gill, P.M.W.; Johnson, B.; Chen, W.; Wong, M.W.; Gonzalez, C.; Pople, J.A. *Gaussian 03, Revision B.05*; Gaussian, Inc. Pittsburgh, PA, 2003.
(30) Biegler-König, F.W.; Schönbom, J. *AIM2000*;, 2.0 ed. Büro für Innovative Software: Bielefeld, Germany, 2002.
(31) Benesi, H.; Hildebrand, J. *J. Am. Chem. Soc.* **1949**, *71*, 2703–2707.